A TIME-BASED CONCEPT FOR TERMINAL-AREA TRAFFIC MANAGEMENT

Heinz Erzberger and Leonard Tobias, NASA Ames Research Center

ABSTRACT

This paper describes an automated air-traffic-management concept that has the potential for significantly increasing the efficiency of traffic flows in high-density terminal areas. The concept's implementation depends on techniques for controlling the landing time of all aircraft entering the terminal area, both those that are equipped with on-board four-dimensional (4D) guidance systems as well as those aircraft types that are conventionally equipped. The two major ground-based elements of the system are a scheduler which assigns conflict-free landing times and a profile descent advisor. Landing times provided by the scheduler are uplinked to equipped aircraft and translated into the appropriate 4D trajectory by the on-board flight-management system. The controller issues descent advisories to unequipped aircraft to help them achieve the assigned landing times. Air traffic control simulations have established that the concept provides an efficient method for controlling various mixes of 4D-equipped and unequipped, as well as low- and high-performance aircraft. Piloted simulations of profiles flown with the aid of advisories have verified the ability to meet specified descent times with prescribed accuracy.

INTRODUCTION

After years of research, automation of air traffic control (ATC) procedures remains a distant goal. While much progress has been made in the processing and display of information for controllers, the major decision and control functions involved in managing traffic continue to be done in the traditional way by teams of controllers who work without significant computer assistance. This situation contrasts sharply with the situation of the pilot of a modern aircraft who uses numerous automated systems for guidance, control, and navigation, including automated flight-path management.

At first, problems in ATC automation often do not appear to be more difficult than typical aircraft guidance and control problems that have been successfully solved. But then, after some promising initial successes, unforeseen problems surface and reach unmanageable complexity as more and more practical constraints are included, leading to the eventual abandonment of the effort. Yet the need to increase safety, capacity, and fuel efficiency, and to reduce controller workload in a period of rising traffic density provides a continued impetus for developing practical solutions to ATC automation problems.

Much of the difficulty in designing automated ATC systems stems from the complex and ever-changing air traffic environment. Whereas controllers usually can adapt to such an environment, automated systems have so far lacked the flexibility to adapt to it. For example, automated systems must be able to handle a range of aircraft types, from high-performance jets to low-performance, general-aviation aircraft. Furthermore, the systems must allow future aircraft equipped with four-dimensional (4D), flight-management systems to fly their optimized flight profiles while efficiently controlling

aircraft with conventional avionics (referred to as unequipped aircraft). Finally, the systems must provide an intelligent interface so the decisions of the automated system can be supervised by the controller.

This paper describes an automated concept for traffic management in the terminal area that has the potential for meeting the design objectives and constraints just discussed. The design evolved from a series of studies in 4D guidance and ATC simulations conducted at NASA Ames Research Center during the past 10 years. The viability of the concept hinges on techniques that accurately control the landing times of all aircraft entering the terminal area, not just 4D-equipped aircraft. The advantage of a system based on time control is that it provides a unified framework for automating flow control and for scheduling and spacing all types of traffic. Furthermore, this time-based system is ideally suited to exploit the time-control capabilities of future 4D-equipped aircraft, whose population in the traffic mix is expected to increase steadily.

The paper begins with an overview of the concept, followed by a review of results from controller-interactive simulations of an initial design. These simulations have shed light on the question of how acceptable the various automated procedures and computer aids are to controllers and how suitable the concept is for controlling a mix of aircraft (e.g., that are equipped and unequipped, high performance and/or low performance). Finally, the design and the piloted-simulator evaluation will be described for an algorithm for controlling the landing time of unequipped aircraft--a crucial element of the concept.

OVERVIEW OF TRAFFIC-MANAGEMENT SYSTEM

Fig. 1 shows the major elements of the terminal-area-traffic-management system that is being studied at Ames Research Center. The two major ground-based elements of this system are primarily embodied in two computer algorithms referred to as the scheduler and the 4D profile descent advisor. The airborne elements are aircraft equipped with 4D flight-management systems and unequipped aircraft.

The scheduler generates the landing order and the conflict-free landing times for all aircraft, both 4D-equipped and unequipped. Primary input to the scheduler is the list of arrivals and their estimated arrival times at the entry point into the extended terminal area. Entry points, also known as feeder fixes, generally are located near the end of cruise flight just prior to the descent point, which is about 120 n.mi. from the destination runway for conventional jet-transport aircraft. The most important factors considered by the scheduler in generating efficient landing times are the minimum separation times between aircraft and the landing-order criterion, as exemplified by the first-come-first-served rule.

The minimum time separations between aircraft are derived from the minimum-distance separation rules specified by the FAA and given in Table 1. These separation rules depend on aircraft weight class (small, large, and heavy) and the landing sequence. By combining the data in Table 1 with the known speed profiles of each aircraft weight class along the common final-approach path, the matrix of minimum time separation (Table 1) can be calculated. If two consecutive aircraft are 4D-equipped, the interarrival

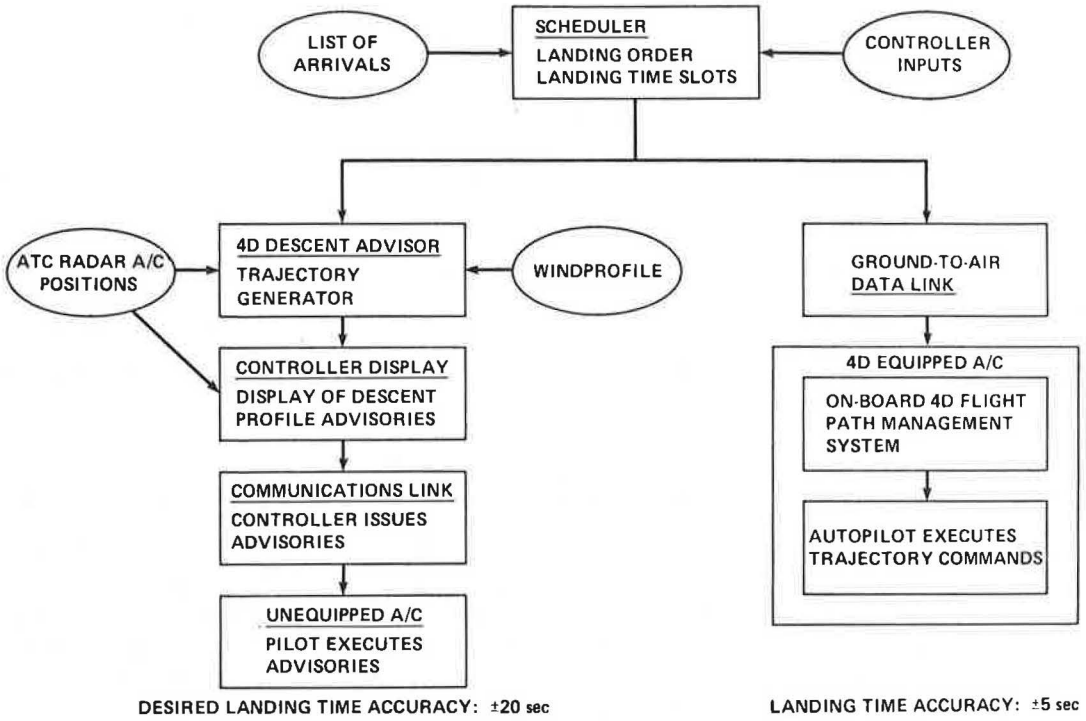

Figure 1 Terminal-Area Traffic Management System

times given in Table 1 are used directly for scheduling purposes. However, unequipped aircraft, which cannot achieve specified landing times as accurately as 4D-equipped aircraft, are given additional time buffers to prevent separation-distance violations. Further discussion of this subject can be found in Ref. 1.

The scheduler is designed as a real-time expert system that provides for efficient interaction with a human controller. The controller monitors the time assignments of the scheduler on a graphics terminal and can override its ordering and time-assignment decisions by using a small, but flexible list of commands. For example, controllers can delay traffic at the feeder fixes or increase the time separation if delays are being encountered in the terminal area. Also, they can overrule the built-in first-come-first-served rule to give landing time priority to a missed approach or emergency aircraft (Ref. 2).

The landing times generated by the scheduler are handled in one of two ways depending on whether the times apply to a 4D-equipped or unequipped aircraft. The times are assumed to be uplinked automatically to equipped aircraft where the on-board 4D flight-management system translates time commands into the appropriate 4D-trajectory commands. The autopilot then flies the aircraft according to these commands, achieving a landing-time accuracy of about $\pm$ 5 sec (Refs. 3,4,).

The landing times for the unequipped aircraft constitute the primary input to the 4D profile descent advisor whose algorithms reside in the ATC host computer or in a minicomputer linked to the host. By using ATC radar-tracking data, wind profiles and aircraft performance models, the descent advisor generates simplified 4D trajectory commands which are displayed on the arrival controller's monitor as brief controller advisories. The arrival controller then issues the advisories

Table 1 DISTANCE- AND TIME-SEPARATION RULES

		Trailing Aircraft					
		Minimum separation distance (n.m)			Minimum separation time (sec)		
Aircraft Type		Small	Large	Heavy	Small	Large	Heavy
First	Small	3	3	3	98	74	74
to	Large	4	3	3	138	74	74
land	Heavy	6	5	4	167	114	94

to the pilot of the unequipped aircraft. When the pilot properly executes these advisories, the unequipped aircraft will arrive at the designated time-control point within acceptable error bounds. The arrival-time accuracy of the unequipped aircraft should be a reasonably small fraction of the minimum inter-aircraft arrival times given in Table 1 in order that the benefits of a time-based system be fully realized. This requirement led to the choice of $\pm$ 20 sec as the desired accuracy.

ATC SIMULATIONS OF MIXED TRAFFIC

The terminal-area traffic-management concept described in the previous section has been evaluated and its design refined in a series of real-time, controller-interactive, ATC simulations. For this purpose an extensive set of software tools and simulation techniques were developed to permit the study of time-based ATC concepts under reasonably realistic conditions. Special features incorporated in the simulator include algorithms for on-board, 4D-guidance and ground-based, speed-advisory systems and interactive scheduling logic with associated graphics displays (Ref. 5).

Examples of critical issues that have been addressed in simulations are the following: 1) Effect of percentage of 4D-equipped aircraft in the traffic mix on controller workload and landing rate; 2) effectiveness of speed advisories; 3) controller procedures for handling 4D-equipped aircraft; and 4) rescheduling of missed-approach aircraft. A complete discussion of simulation results can be found in Refs. 2 and 6. The simulation scenario and controller procedures will be briefly described first.

Scenario and Controller Procedures

The terminal area simulated in these studies is based on the John F. Kennedy (JFK) International Airport in New York. The route structure and runway configuration together with information used by the controllers are shown in Fig. 2. Two routes, Ellis from the north and Sates from the south, are high-altitude routes flown by large and heavy jet-transport aircraft. Both 4D-equipped and unequipped aircraft fly profile-descent, fuel-conservative procedures, providing a mix of the same speed class on the same route. Low-performance (general-aviation) aircraft fly the Deerpark route from the east, but use the same final approach and land on the same runway as

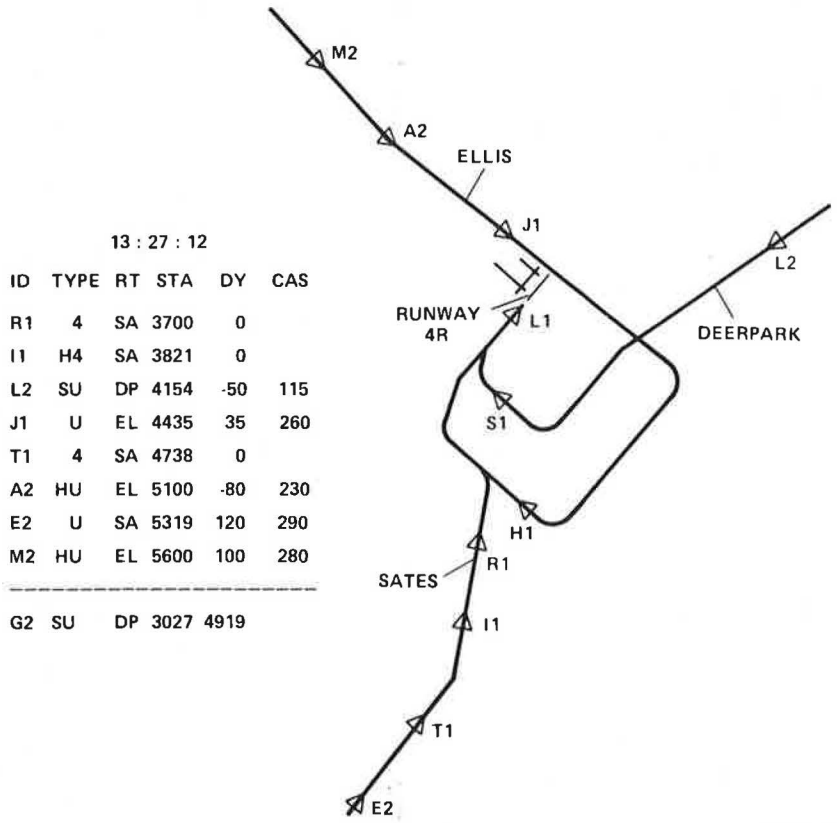

Figure 2 Controller Display Showing Route Structure and Flight-Data Table

the jet traffic. The Deerpark traffic is unequipped and always constitutes 25% of the traffic mix.

In these simulations aircraft entered the extended terminal area at the feeder fix points flying at cruise speed and altitude. The total distance to be flown by high-performance jets was 120 n.mi. and that flown by low-performance aircraft was 60 n.mi. Two air traffic controller positions were established, arrival control and final control. The arrival controller controlled aircraft from all three feeder fixes and transferred traffic to the final controller at approximately 30 n.mi. from touchdown.

Control procedures differed for 4D-equipped and -unequipped aircraft. Controllers were instructed to monitor the progress of 4D-equipped aircraft after the time assignment had been established, and to override the automated scheduler only if necessary to ensure safe separation. Any 4D-equipped aircraft could also be controlled by conventional methods and treated as unequipped. Alternatively, a 4D-equipped aircraft that had been taken off its 4D route and time schedule could be given a waypoint to recapture a 4D route and be given a revised landing time. Unequipped aircraft were considered to be navigating in the conventional manner via very-high-frequency omnidirectional range procedures, with altitude clearances, radar vectors, and speed control.

A typical arrival controller display is shown in Fig. 2. The map portion of the display provides a horizontal display of traffic in the terminal area. Each aircraft position is shown by a triangular symbol.

aircraft identification, type, altitude, and speed. The information in the flight data table in the upper-left portion of the display is generated by the scheduler and speed advisory system. At the top of the table, the time is shown in hours, minutes, and seconds. The first column shows the aircraft identification (ID), such as "R1." The second column provides aircraft type (TYPE) which includes 1) weight category [small (S), large (blank), or heavy (H)] and 2) 4D status [equipped (4) or unequipped (U)]. The third column provides the assigned route (RT). The fourth column is the scheduled time of arrival (STA) at the runway in minutes and seconds. Thus, R1 is scheduled to touch down at 13:37:00. Note that touchdown times are shown for all aircraft, whether they are 4D-equipped or unequipped. For the 4D-equipped aircraft, these times are assigned by the ground-based computer system. For the unequipped aircraft, the time assignments are not given to the pilot directly; rather, the controller uses speed advisories and known-to-be-on-time positions of 4D-equipped aircraft as they traverse their routes to achieve touchdown at the times indicated. The next column is the expected delay (DY) at touchdown in seconds. In an effort to simulate the characteristics of the current en-route ATC system, which does not provide accurate time control, the unequipped aircraft were assumed to depart their feeder fixes with an initial time error uniformly distributed in the range $\pm$ 120 sec. This amount is considered rather large even by today's controller experience and certainly will be less with a future en-route metering system. Thus, if an aircraft departed the feeder fix 90 sec late, a DY of 90 would be displayed, indicating that unless controller action were taken, the aircraft would touch down 90 sec late. Early arrivals were indicated by a negative value in the DY column, and late arrivals by a positive value. All 4D-equipped aircraft can meet time schedules within $\pm$ 5 sec; hence, these small errors were neglected (Refs. 3,7).

The data in the last column give the calibrated airspeeds (CAS) in knots, computed by the speed advisory system. These speed advisories, which are based on current aircraft position, altitude, and wind profile, help the controller to correct the unequipped aircraft's time errors shown in the DY column. The speed advisory is recomputed once per minute using the current aircraft position as long as the delay remains larger than 20 sec. This feature gives the arrival controller the freedom to issue the advisory at a convenient time.

The speed advisory incorporated in the ATC simulation is a simplified early version of the more recently developed descent-advisor algorithm, which is detailed in a later section. It will be seen that the new algorithm also provides top-of-descent-point and Mach number advisories in addition to the CAS advisory. However, for investigating controller response and other ATC-related issues the speed advisory system used provides a sufficiently realistic substitute.

Finally, aircraft below the dotted line in Fig. 2 are aircraft that will enter the simulated control region at their respective feeder fixes within the next 5 min. The feeder-fix start times are given in minutes and seconds.

Summary of Results

The traffic mixes examined in simulation runs, each lasting 1.5 hr, were 0%, 25%, and 50% 4D-equipped aircraft. For each mix, the total arrival rate

from the three approach routes was selected to generate a full landing schedule with no excess time gaps between touchdown. This condition required arrival rates that varied from 30 aircraft/hr for the 0% baseline mix to 33 aircraft/hr for the 50% mix. The variation is due to the time separation buffers added for the unequipped aircraft. All runs included the $\pm$ 120-sec feeder-fix departure errors for unequipped aircraft.

Controllers rated all mixes as having acceptable workload, but considered the 25% mix without speed advisories the most difficult to control. This result was probably related to the controller procedures adopted for this experiment of not disrupting the planned 4D paths of the equipped aircraft unless it was necessary for safety. As a consequence, the final controller occasionally vectored an unequipped aircraft to control its distance spacing from an equipped aircraft when he would have preferred under the circumstances to vector the equipped aircraft. One solution to this problem that will be examined in future simulations is a relaxation of the "do not disrupt" rule. Then, after vectoring an equipped aircraft, the controller would assign a new 4D route and landing time to that aircraft. Some experience with this approach was recently obtained in handling missed approaches of equipped aircraft (Ref. 2).

Controllers regarded the baseline mix of 0% as reasonable with respect to control difficulty, but not because of lightened workload. Rather, it was the most familiar mode of operation. The controllers regarded the 50% mix as easiest to control.

Under all mix conditions, controllers found the landing order provided by the flight-data table in Fig. 2 to be helpful and generally accepted the suggested ordering. But they did not make use of the numerical landing-time data.

Further insight into the simulation results can be obtained by examining the composite plot of aircraft ground tracks generated during a 1.5 hr simulation run. Such a plot is shown in Fig. 3a for the 25% mix without speed advisories. In the arrival sector, from the feeder fixes to the hand-off points, the flightpaths are largely undisturbed, indicating that the arrival controller acted primarily as a traffic monitor. After the hand-off points, the flightpaths spread into the broad envelope that characterizes manual vectoring. This spreading is the result of the final controller issuing heading vectors that cause unequipped aircraft merging from the three routes to be properly spaced on final approach. Although the arrival controller had available the scheduled landing times for the unequipped traffic, he could not use this information to correct spacing errors before the hand-off point. Evidently, aircraft are still too far from the merge point for the arrival controller to anticipate future spacing errors. As a result, control difficulty and workload were unevenly distributed between the two control positions, with the final control position requiring higher skill and greater workload than the approach control position.

The composite plot for the 25%-mix condition, in which speed advisories were2used, is shown in Fig. 3b. The advisories were issued by the approach controller shortly after unequipped aircraft with time errors exceeding 20 sec departed the feeder fixes. Typically, only one advisory was issued per aircraft. The unequipped traffic was handed off to the final controller with significantly reduced time errors. As a consequence, the final controller

needed to make only minor adjustments in the flightpaths to achieve the desired spacing. The resulting improvement in the traffic flow manifests itself as a reduction in the spread of flightpaths along all three routes. Furthermore, controllers commented that speed advisories resulted in less bunching of traffic and fewer "ties" in the merging area. Traffic seemed to blend together smoothly and required fewer vectors, resulting in reduced complexity of control.

The 50% mix with speed advisories was rated by controllers as providing the most desirable control environment of all conditions evaluated. The controllers commented that it was easy to fit the unequipped aircraft into their planned time slots by vectoring or speed control in the final control sector. One controller stated that he could work and stay on top of the traffic without being overtaxed. These favorable controller evaluations are reflected in the well-ordered and narrowly distributed composite-trajectory plots (Fig. 3c) obtained for this simulation run.

In conclusion, the procedures, computer assets, and information displays used in these simulations established a workable baseline configuration for efficiently controlling a mix of 4D-equipped and unequipped aircraft in a time-based environment.

DESIGN AND SIMULATION OF 4D-PROFILE-DESCENT ADVISOR

The following sections present the theory of design and the results of a piloted simulation of the descent advisor algorithm. The primary topics covered in the discussion of the design included selection of descent procedures, derivation of the aircraft equations of motion, the method of numerical integration, and an example output from the computer implementation of the algorithm.

Selection of Descent Profiles

The trajectories generated by the descent-advisor algorithm are based on models of fuel conservative procedures used in airline operations. In such procedures, the pilot first selects the point of descent using a simple rule of thumb to estimate the idle-thrust descent distance. A rule frequently used by pilots assumes 300-ft altitude loss/n.mi. Choosing the point of descent so as to minimize level flight at low altitude is probably the pilot's most important decision for optimizing fuel efficiency. At the point of descent, the pilot reduces thrust approximately to idle and at the same time commands a pitch-down attitude so as to hold Mach number fixed at the cruise value. Thrust may be kept slightly above the idle position if there is a requirement not to exceed a descent-rate limit, typically 3000 ft/min. During this constant Mach descent, CAS will increase steadily. When CAS has climbed to a desired value, the pilot ceases holding the Mach number and begins tracking the desired CAS through appropriate adjustments to the pitch attitude. As the aircraft approaches an altitude of 10,000 ft, the pilot reduces the descent rate briefly to decelerate to 250 knots calibrated airspeed (KCAS) as required by ATC regulation. If the initial descent point had been selected properly, the aircraft will be 30 n.mi from touchdown at the end of the deceleration and the pilot will resume the descent into the terminal area.

The primary function of the descent-advisor algorithm is to select the speed profile that achieves the arrival time specified by the scheduler.

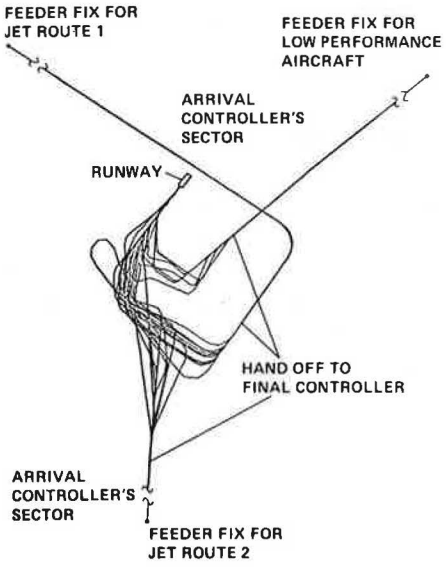

(a) 25% 4D Equipped; no speed advisories for unequipped

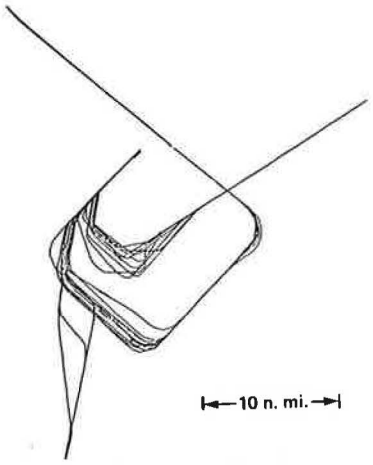

(b) 25% 4D equipped; speed advisories for unequipped

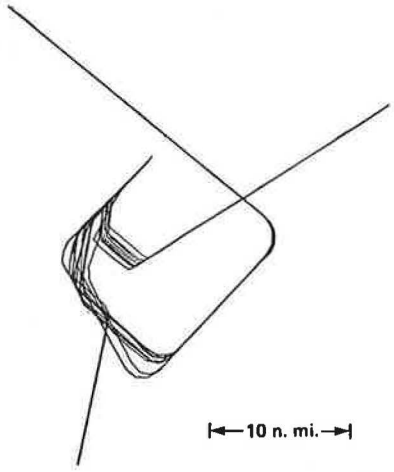

(c) 50% 4D equipped; speed advisories for unequipped

Figure 3 Composite Trajectories From ATC Simulation

A secondary function of the advisor is to provide an accurate estimate of the point of descent to optimize fuel efficiency. Later it will be seen that the algorithm accomplishes both functions in a unified computational procedure.

The algorithm selects the speed profile with the help of a parameter, σ which determines a Mach number and CAS that falls within the speed envelope of the aircraft as follows:

$$M = M_{min} + \sigma(M_{max} - M_{min}) ; \quad 0 \leq \sigma \leq 1 \tag{1}$$

$$V_{CAS} = V_{min} + \sigma(V_{max} - V_{min}) \tag{2}$$

The family of speed profiles generated by Eqs. (1) and (2) are superimposed in Fig. 4 upon the speed envelope of a 727 aircraft. Note that the maximum- speed boundary contains a corner at 25,000 ft where the maximum Mach number and maximum CAS boundaries intersect. The family of speed profiles generated by Eqs. (1) and (2) converges into this corner as σ approaches 1, thereby covering the full-speed envelope of the aircraft.

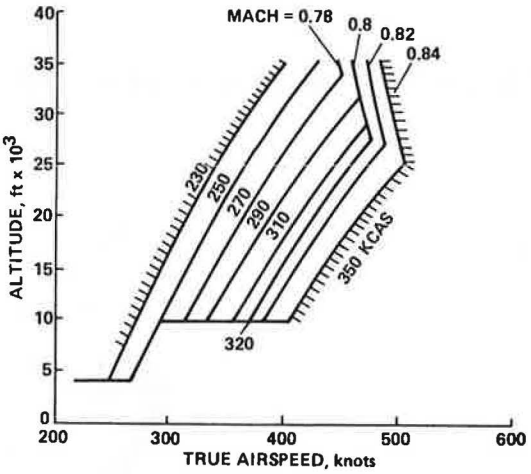

Figure 4 Speed Profiles for Time Control

The relationship between the parameter, σ and the arrival time at the 30 n.mi. from touchdown point is not amenable to a closed-form solution, since there are complex aerodynamic, propulsion, and atmospheric models embedded in the relationships. Thus, a procedure that computes σ iteratively has been developed. Initially, the procedure calculates the minimum and maximum arrival=times by setting σ to one and zero, respectively. If the specified time falls within the feasible time range, iteration on σ by a directed trial and error technique is begun and continues until the arrival- time error falls within acceptable bounds (for example, 2 sec). Experience has shown that five iterations are generally sufficient to achieve a 2-sec accuracy. The next section will describe the equations of motion that must be integrated for each iteration of σ. (Ref. 4).

For reasons of brevity, the speed-profile selection process just described has been considerably simplified compared to the method actually implemented in the computer algorithm. The computer algorithm includes a more complicated mapping of σ into profiles that provides an appropriate transition from the

cruise Mach number to the descent Mach number. It also eliminates constant Mach segments in the speed profile if the descent CAS is less than cruise CAS.

Equations of Motion

Numerical integration of a simplified set of point-mass equations of motion has been adopted as the basic method for calculating the descent trajectory and arrival time corresponding to a given speed profile. This method is computationally intensive, but it is more flexible and more accurate than schemes that depend on analytical approximations or precomputations of trajectories. Here, no restrictive assumptions on pilot procedures, wind profiles, or aircraft performance models need be made in calculating trajectories. Potentially, it would even be possible to include the preferred procedures of individual airlines in the calculations of the descent trajectories.

To begin with, it is assumed that the aircraft is flying along a known horizontal path in space. Therefore, the problem simplifies to finding the vertical profile along the known horizontal path. Furthermore, the horizontal path is assumed to be a straight line, though it is easily modified to include curved segments. Using an Earth-fixed coordinate system with x as the horizontal axis pointing in the flight direction and h as the upward-pointing vertical axis, the components of inertial velocity u and w that must be integrated are:

$$\frac{dx}{dt} \equiv u = V_T \cos \gamma_a + u_w \equiv F_1 \tag{3}$$

$$\frac{dh}{dt} \equiv w = V_T \sin \gamma_a \equiv F_2 \tag{4}$$

where V_T is the true airspeed, γ_a the aerodynamic flightpath angle and u_w the horizontal component of wind. The airspeed acceleration is calculated from the following equations:

$$\frac{dV_T}{dt} = \frac{(T - D)}{m} - g \sin \gamma_a - \frac{du_w}{dt} \tag{5}$$

$$mV_T \frac{d\gamma_a}{dt} = L - mg \cos \gamma_a = 0 \tag{6}$$

where T is thrust, D is drag, L is lift, m is aircraft mass, and g is acceleration of gravity. The approximation in Eq. (6) implies that accelerations normal to the flightpath are considered to have negligible effect on trajectory modeling for this application. This assumption is valid for the low-g maneuvers encountered in commercial transport operations. The value of lift computed by solving the algebraic Eq. (6) couples into Eq. (5) through the dependence of drag on lift. The last term in Eq. (5) reflects the influence of a time dependent wind, also known as wind shear, on the airspeed acceleration. On the time and distance scale of a descent trajectory, it is reasonable to assume that wind shear is only encountered during changes in altitude, implying the relationship $u_w(h)$. The drag coefficient involved in calculating the

drag force was represented by seven fourth-order polynomial functions, each representing a different Mach number in small increments from Mach 0.6 to 0.9. Both tables and polynomial functions were used to model the thrust and the fuel flow as a function of engine-pressure ratio (EPR), Mach number, temperature, and pressure. Idle thrust and fuel flow were stored in separate tables indexed by Mach number and altitude. Such aircraft performance models must be developed for all major aircraft types that operate into the terminal area where the descent advisor is used to provide time control.

Another important quantity that the descent advisor uses in computing trajectories is aircraft mass. An adequate estimate of mass can be calculated from a knowledge of aircraft type, point of origin, and takeoff mass. Such information is generally contained in aircraft flight plans or can be obtained from the pilot at take-off time.

Constant Mach/Constant CAS Segments

In modeling the speed profile, it was shown that pilots maintain either a constant Mach number or a constant CAS during the majority of an aircraft's descent into the terminal area. This assumption can be used to reduce the differential equation for airspeed, Eq. (5), to an algebraic relation. Consequently, only the position rates, Eq. (3) and (4), need to be numerically integrated in such segments.

Considering first the constant Mach segment, one can write from the definition of Mach number

$$V_T = a(h)M \tag{7}$$

where a is the speed of sound, which is a function of altitude. Differentiating this equation with respect to time and using the fact that M is constant, yields

$$\frac{dV_T}{dt} = M \frac{da}{dh} \cdot \frac{dh}{dt} = M \frac{da}{dh} \gamma_a V_T \tag{8}$$

where use was made of Eq. (4) and $\sin \gamma_a \simeq \gamma_a$. After replacing the left side of Eq. (5) with the right side of Eq. (8) and calculating the wind shear term in Eq. (8) as $du_w/dt = (du_w/dh)\ \gamma_a V_T$, an explicit expression γ_a is obtained as

$$\gamma_a\Big|_{M \text{ constant}} = \frac{(T - D)}{m} \cdot \frac{1}{\left(M \frac{da}{dh} V_T + g + \frac{du_w}{dh} V_T\right)} \tag{9}$$

where the small angle approximation, $\sin \gamma_a \simeq \gamma_a$ has been used. For a constant Mach segment at a known altitude, all quantities needed to compute γ_a are either known or measurable. The derivative da/dh must be computed by differentiation of the speed of sound function. If this function is obtained from a table of the standard atmosphere, the derivative can be precomputed numerically, curve-fitted for the range of altitudes of interest, and

permanently stored for use by the program. However, the most accurate results will be obtained by calculating the speed of sound function from the temperature profile measured at the time and location of the descent. Calculation of the wind shear term, du_w/dh, depends on knowledge of the altitude-dependent wind profile in the descent airspace. The descent advisor must compute the derivative numerically and update the derivative whenever the wind profile is updated. Thus, each terminal area where the descent advisor is used will have to provide for measuring the wind profile at regular intervals during each day. Several technical means exist for measuring the wind profile, including the use of conventional weather balloons. (Ref. 8).

Considering next the constant CAS segment, an expression for γ_a can be derived in a similar manner. One begins by writing the expression relating true airspeed and CAS

$$V_T = V_T(V_{CAS}, h) \tag{10}$$

The time derivative of Eq. (10) yields a relation analogous to that for the constant Mach case

$$\frac{dV_T}{dt} = \frac{dV_T(V_{CAS}, z)}{dh} \quad V_T \sin \gamma_a \tag{11}$$

An explicit expression for $V_T(V_{CAS}, h)$ in terms of V_{CAS}, the speed of sound, a, and the atmospheric pressure, p, can be derived from expressions found in standard textbooks on aerodynamics and flight mechanics (Ref. 9)

$$V_T = a\sqrt{\frac{2}{\gamma_{air}-1}\left[\left(\frac{p_{SL}}{p}\left[\left(\frac{\gamma_{air}-1}{2\gamma_{air}}\frac{\rho_{SL}}{p_{SL}}V_{CAS}^2+1\right)^{\frac{\gamma_{air}}{\gamma_{air}-1}}-1\right]+1\right)^{\frac{\gamma_{air}-1}{\gamma_{air}}}-1\right]} \tag{12}$$

where p_{SL} and ρ_{SL} are sea-level values of atmospheric pressure and air density, respectively, and γ_{air} is the specific heat of air. Since atmospheric pressure, p, and speed of sound, a, are known functions of altitude, h, the expression for V_T in Eq. (12) is in the form required by Eq. (10). However, the complexity of Eq. (12) makes it infeasible to compute the derivative of V_T with respect to h analytically for use in Eq. (11). Therefore, the derivative is computed by a standard numerical technique.

The expression for the flightpath angle in the constant CAS segment can now be obtained by combining Eqs. (5) and (11)

$$\gamma_a\Big|_{CAS\ constant} = \left(\frac{T-D}{m}\right)\frac{1}{\left(V_T\frac{dV_T}{dh}+g+\frac{du_w}{dh}V_T\right)} \tag{13}$$

The last question to be settled in computing γ_a is how to determine the thrust, T, in the two expressions for the flightpath angle. In a conventionally equipped aircraft, pilots hold thrust more or less constant during descent by keeping the throttle levers at their idle position. However, if the idle throttle position results in an excessive descent rate during a portion of a descent, the pilot will adjust the throttles to maintain the

descent rate at a specified limit. Since both specified-thrust and specified-descent-rate segments can occur under appropriate conditions, both have been implemented and the choice between them is determined by the constraints of the descent. If the descent rate, $\dot{h}$ is specified, γ_a is computed from the relation $\gamma_a \simeq \dot{h}/V_T$ and Eqs. (9) and (13) are solved for the unknown thrust. It should be noted here that a pilot cannot easily fly a commanded value of γ_a directly because no readout of this quantity is provided on conventional cockpit instruments.

It is of interest to evaluate the effect of windshear term, $(du_w/dh).V_T$ on the descent profile. For example, a decreasing tail wind $(du_w/dh > 0)$ during descent results in a γ_a that is shallower than that for a constant wind. Thus, in this case, the descent trajectory experiences an expansion of the distance to descend from cruise altitude. The opposite effect occurs for a decreasing head wind. For a typical wind shear of 2 knots/1000 ft, the calculated distance to descend from 35,000 ft to sea level would be in error by 5 n.mi. if this term were neglected.

Integration Algorithm

A fourth-order Runge-Kutta scheme was adopted for the numerical integration of the trajectory equations (Ref. 10). This scheme gives accurate results with relatively large step sizes and also does not require evaluating derivatives of the complex functions appearing on the right-hand sides of the equations being integrated. The latter property simplifies the integration of functions specified in tabular form. For the constant Mach number and constant CAS segments, which constitute the majority of the descent, only Eqs. (3) and (4) need to be integrated, as previously explained. Letting Δt represent the time increment, then the states (x_{i+1}, h_{i+1}) at the (i+1)st time increment are determined from four sets of sequentially computed state increments as follows:

$$\Delta_1 x_i = (\Delta t) F_1(x_i, h_i, t_i) \tag{14}$$

$$\Delta_1 h_i = (\Delta t) F_2(x_i, h_i, t_i) \tag{15}$$

$$\Delta_2 x_i = (\Delta t) F_1\left(x_i + \tfrac{1}{2}\Delta_1 x_i, h_i + \tfrac{1}{2}\Delta_1 h_i, t_i + \tfrac{1}{2}\Delta t\right) \tag{16}$$

$$\Delta_2 h_i = (\Delta t) F_2\left(x_i + \tfrac{1}{2}\Delta_1 x_i, h_i + \tfrac{1}{2}\Delta_1 h_i, t_i + \tfrac{1}{2}\Delta t\right) \tag{17}$$

$$\Delta_3 x_i = (\Delta t) F_1\left(x_i + \tfrac{1}{2}\Delta_2 x_i, h_i + \tfrac{1}{2}\Delta_2 h_i, t_i + \tfrac{1}{2}\Delta t\right) \tag{18}$$

$$\Delta_3 h_i = (\Delta t) F_2\left(x_i + \tfrac{1}{2}\Delta_2 x_i, h_i + \tfrac{1}{2}\Delta_2 h_i, t_i + \tfrac{1}{2}\Delta t\right) \tag{19}$$

$$\Delta_4 x_i = (\Delta t) F_1(x_i + \Delta_3 x_i, h_i + \Delta_3 h_i, t_i + \Delta t) \tag{20}$$

$$\Delta_4 h_i = (\Delta t) F_2(x_i + \Delta_3 x_i, h_i + \Delta_3 h_i, t_i + \Delta t) \tag{21}$$

$$x_{i+1} = x_i + \frac{1}{6}(\Delta_1 x_i + 2\Delta_2 x_i + 2\Delta_3 x_i + \Delta_4 x_i) \quad (22)$$

$$h_{i+1} = h_i + \frac{1}{6}(\Delta_1 h_i + 2\Delta_2 h_i + 2\Delta_3 h_i + \Delta_4 h_i) \quad (23)$$

At the top and bottom of the descents, rapid changes in speed occur, and neither Mach number nor CAS remain constant. During these acceleration or deceleration intervals it is also necessary to integrate Eq. (5) representing rate of change of airspeed. The incremental Eqs. (14) through (23) were augmented appropriately to integrate this equation.

The integration time increment, Δt, was experimentally selected to be as large as possible to consistently give accurate and numerically stable results. The optimum step sizes were 60 sec for the constant Mach/constant CAS segments and 30 sec for the acceleration/deceleration segments.

Example Descent Profile

This section gives an example of a complete descent profile generated by the program. The aircraft model used is that of a 727-200 weighing 140,000 lb at the start point. Initially the aircraft is cruising at Mach 0.8 and 35,000 ft and is 150 n.mi. from touchdown. The time-control point is located 30 n.mi. from touchdown at 10,000-ft altitude. At this point, the aircraft must have completed its deceleration to 250 knots. A descent time of 985 sec, measured from the 150 n.mi. starting point to the end of deceleration, is specified. The wind is assumed to be zero throughout the descent.

The synthesized trajectory consists of four segments whose parameters are given in Table 2. The first segment is a level-flight segment leading from the starting point to the point of descent at 98 n.mi. from touchdown. The second segment is a Mach 0.8 descent with EPR, which controls thrust, set to near idle (approximately 1). The third segment begins at 27,603 ft where Mach 0.8 corresponds to a CAS of 320 knots. A descent time of 985 sec, measured from the 150 n.mi. starting point to the end of the deceleration, is specified. The wind is assumed to be zero throughout the descent.

The synthesized trajectory consists of four segments whose parameters are given in Table 2. The first segment is a level-flight segment leading from the starting point to the point of descent at 98 n.mi. from touchdown. The second segment is a Mach 0.8 descent with EPR, which controls thrust, set to near idle (approximately 1). The third segment begins at 27,603 ft where Mach 0.8 corresponds to a CAS of 320 knots. In this constant CAS segment, thrust is held at idle. The fourth segment consists of deceleration from 320 to 250 knots at 10,000 ft. The last line of data in the fourth segment shows that the time and the distance to touchdown closely match the specified values. Various other parameters relating to the trajectory synthesis such as the number of integration steps in each segment and the fuel consumed are also included in the table.

In addition to achieving the specified descent time, the synthesized trajectory is also relatively fuel efficient, requiring only 1208 lb for all four segments. Good fuel efficiency is assured by the combined benefits of an idle-thrust descent and the choice of descent point that results in the

TABLE 2 EXAMPLE OF SYNTHESIZED PROFILE

Comments	Time (sec)	Dist. (n. mi.)	Altitude (ft)	Mach	V_T (knots)	V_{CAL} (knots)	EPR	Thrust (lbs)	Fuel (lbs)	Alt Rate (ft/min)
	Cruise, two integration steps									
Step size = 500 sec Capture = 98.4 n. mi	0.0 402.5	150.0 98.4	35000 35000	0.80 0.80	461 461	272 272	1.95 1.95	9824 9824	0 867	0 0
	Constant Mach, four integration steps									
Step size = 60 sec Mach, constant Vertical speed, constant Capture = 320 KCAS	402.5 462.5 522.5 550.4	98.4 90.6 82.8 79.1	35000 32000 29000 27603	0.80 0.80 0.80 0.80	461 467 473 476	272 291 310 319	1.06 1.09 1.13 1.14	1597 2173 2945 3363	867 906 954 981	0 -3000 -3000 -3000
	Constant CAS, nine integration steps									
Step size = 60 sec CAS, constant EPR, constant Capture = 10,000 ft. alt.	550.4 610.4 670.4 730.4 790.4 850.4 910.4 928.4	79.1 71.4 63.9 56.8 50.0 43.4 37.1 35.2	27603 24665 21781 18952 16172 13448 10785 9999	0.80 0.76 0.72 0.68 0.64 0.61 0.58 0.58	476 455 436 418 402 386 372 367	319 319 319 319 319 319 319 319	1.00 1.00 1.00 1.00 1.00 1.00 1.00 1.00	73 -148 -301 -377 -353 -316 -297 -299	981 1008 1035 1063 1092 1124 1160 1172	-3000 -2912 -2854 -2807 -2752 -2693 -2637 -2621
	Bottom-of-Descent Deceleration, three integration steps									
Step size = 30 sec Mach, CAS not constant Vertical speed, constant EPR, constant Capture = 250 KCAS	928.4 958.4 986.5	35.2 32.3 30.0	9999 9999 9999	0.58 0.51 0.45	367 324 288	319 281 249	1.00 1.00 1.00	-299 -125 17	1172 1191 1208	0 0 0

termination of the trajectory exactly at the specified altitude and distance from touchdown.

Piloted Simulator Evaluation: Experimental Setup

An evaluation of the descent advisor concept was conducted on a so-called phase II simulator of a 727-200 aircraft located in the Man-Vehicle Systems Research Facility at Ames Research Center. This simulator, manufactured by Singer-Link, is widely used by airlines for crew training. The simulator is equipped with a six-degree-of-freedom motion system and a night/dusk vision system. Computer-generated imagery of the night or dusk scene is displayed in front of the cockpit windows by four projectors which give a wide, high-resolution field of view to the pilot and copilot.

Each simulated flight consisted of a straight-in approach beginning 150 n.mi. from the runway threshold at an altitude of 35,000 ft and a speed of Mach 0.8. In all flights, a tail wind of 70 knots at 35,000 ft decreasing linearily to zero at the runway was simulated. Simulated weather conditions consisted of a visibility ceiling of 1000 ft above the runway, with tops at 5000 ft and light turbulence at all altitudes. Pilots were briefed on wind and weather conditions prior to the simulation runs.

Test subjects were three current 727 pilots, one each from three major U.S. airlines. Initially, each pilot was asked to fly his own airline-recommended descent profile, which will be referred to as the baseline profile. The three pilots chose essentially the same baseline profile, consisting of a Mach-0.8/280-KCAS descent. Each pilot also estimated his top-of-descent point using the 300 ft/mi rule of thumb mentioned earlier. Range to touchdown was provided by a standard cockpit readout of distance measuring equipment (DME) range from a station located at the destination airport. All baseline profiles were flown without ATC advisories.

After completing the baseline descents, the pilots flew three types of controller-assisted descents referred as nominal, slow, and fast with speed profiles of Mach 0.8/320 KCAS, 230 KCAS, and Mach 0.85/350 KCAS, respectively. Note that the slow and fast profiles follow the limits of the speed envelope for this aircraft (Fig. 4).

Before flying these profiles in the simulator, pilots received brief, written instructions on operational techniques to be used:

1) Thrust Management. - The flight idle position is to be used in tracking the speed profile unless the descent rate exceeds 3000 ft/min. If such is the case, add only sufficient thrust to keep the descent rate from exceeding 3000 ft/min.

2) Deceleration at the Top (Slow Profile). - First, reduce thrust to idle at the descent-procedure start point; second, maintain level flight (zero descent rate) while decelerating to the specified CAS; and third, begin the descent as the specified CAS is approached.

3) Acceleration at the Top (Fast Profile). - At the descent-procedure start point (the top of descent point in this case) initiate a pitch-down maneuver to achieve a 3000-ft/min descent rate. Then, maintain cruise thrust while accelerating; as the specified Mach number is approached, reduce thrust according to 1).

4) Deceleration at the Bottom of Descent (Nominal and Fast Profiles). - As the aircraft approaches 10,000-ft altitude, decelerate to 250 KCAS in level flight and with thrust still at idle resume descent at the 30 n.mi. to the touchdown point.

The descent advisories were issued during the simulation by a pseudo-controller located at the engineer's position in the cockpit. The advisories were issued only once approximately a minute before the start point of the procedures and specified the DME range of the start point and the speed profile. Calculated off-line by the previously described computer program, the advisories typically contained the following information, "Begin descent procedure at 108 DME; follow a Mach 0.8/320 speed profile using idle thrust."

Each type of controller-assisted descent was flown four to six times. These few simulation runs are believed to provide sufficient information to determine the feasibility of the concept. However, they are too few in number to warrant extensive statistical analysis of the results.

Discussion of Results

Errors in the predicted time of descent measured at the time-control point were the principal criterion for evaluating the effectiveness of the controller-assisted (and computer-generated) profile descent advisories. Also, the instantaneous-altitude and time-tracking errors as well as the fuel efficiency of the descents provide important measures of effectiveness. Finally, the pilots participating in the simulation were asked to comment on the value and acceptability of the advisories. This simulation focused on isolating errors attributable to pilot technique. Errors caused by other sources such as wind and aircraft-model uncertainties can be determined more efficiently by analysis and fast-time simulation, and therefore are not addressed here.

The results for the various types of descents are given in Figs. 5 through 8 as composite plots of time and altitude versus range to touchdown. Figure 5 shows the composite plots for four baseline descents. Although all pilots presumably used the same procedure to fly their profiles, the data revealed significant time and altitude variations between profiles, reflecting differences in individual pilot technique. At 30 n.mi. from touchdown time-control point, the variability in time is 196 sec. Here, variability is defined as the difference between the earliest and latest arrival time for all profiles of a particular type and is used as a conservative substitute for standard deviation.

Since the typical landing-time interval between aircraft is approximately 100 sec (Table 1), a 196-sec error range implies difficulties in achieving efficient traffic flow at terminal areas where two or more streams of aircraft flying unaided profile descents are merged. Thus, unaided aircraft assigned conflict-free time slots at the top of descent by an en-route metering system would accumulate unacceptable time errors during the descent, and would therefore not be conflict free at the merge point. As a result, the controller would frequently have to interrupt the profile descents to resolve potential conflicts and ensure efficient traffic flow. Such problems have indeed been experienced in ATC simulations of unaided profile descents (Ref. 11) and are also evident in the results of the ATC simulations discussed earlier.

As shown in the composite plots in Fig. 6, the time variability of the nominal profile descents, flown with the aid of the descent advisories, is reduced from 196 sec for the baseline descents to only 35 sec. Furthermore, the scatter in the altitude profiles is significantly reduced throughout the descent. The predicted trajectory with an arrival time of 893 sec at 30 n.mi. is also plotted in Fig. 6, but is difficult to distinguish from the simulated trajectories because of crowding of the plots. These improvements in accuracy clearly demonstrate the advantage of using the advisories. With the top-of-descent point specified, pilots could concentrate on tracking the speed profile and needed to pay little attention to thrust and altitude management. Without advisories, pilots often cross-check altitude and range and then read just the thrust so as to minimize anticipated altitude errors at the bottom of the descent. With the advisories, pilots could maintain thrust at idle throughout, and yet be confident that the altitude target at 30 n.mi. would be achieved.

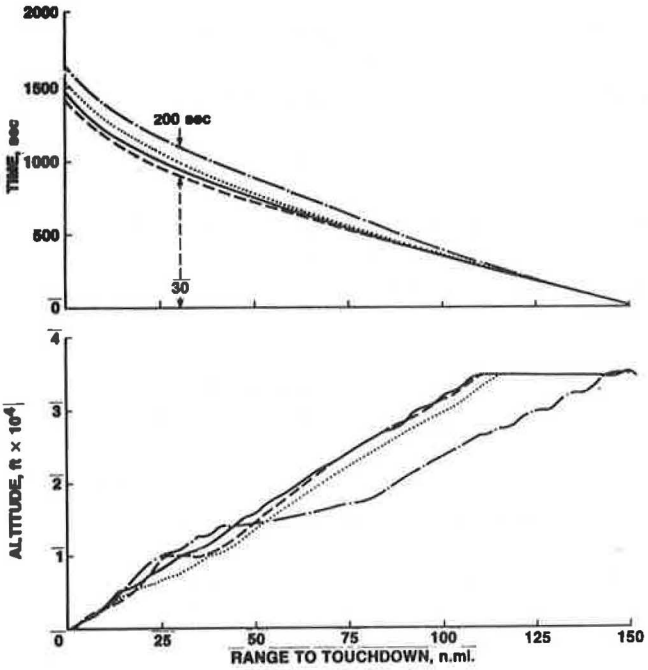

Figure 5 Baseline Descents

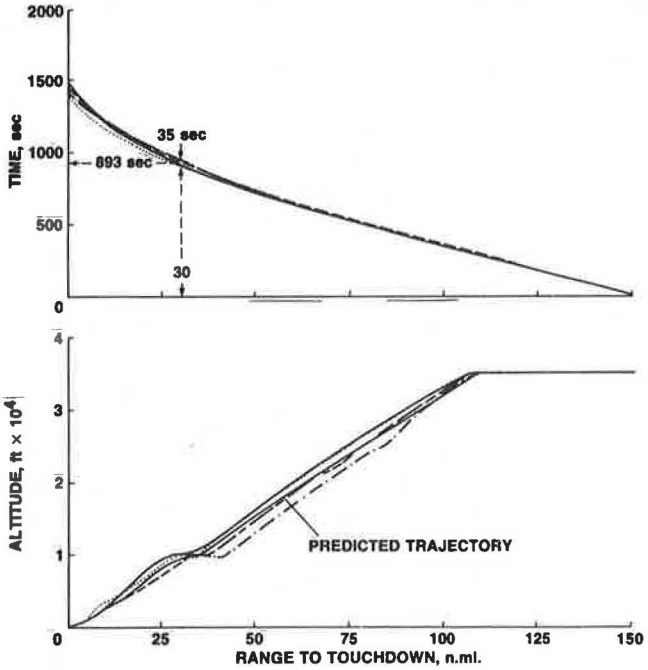

Figure 6 Nominal Decents: 0.8/320

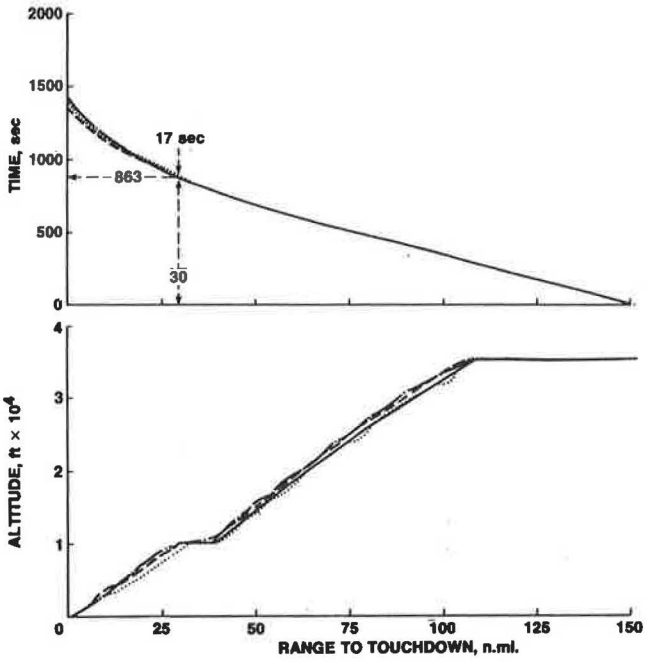

Figure 7 Fast Descents: 0.84/350

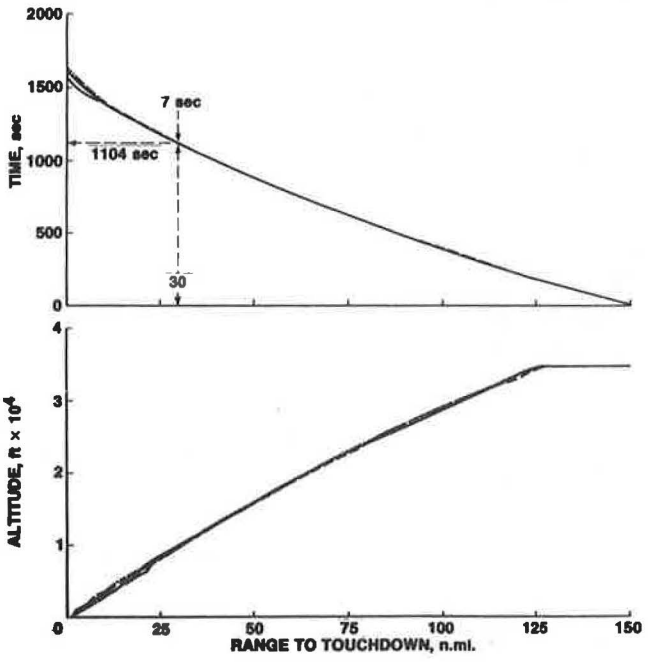

Figure 8 Slow Descents: 230

As seen in the composite plots, Figs. 7 and 8, the time variability and the altitude scatter of the fast and slow profiles are even lower than those of the nominal profile. In fact, the slow profiles have the unusually low variability of only 7 sec, which one would expect to obtain only from a closed-loop 4D guidance system. This high accuracy is probably related to the fact that they are simpler to fly than the other two types of profiles. The slow profiles are flown at a constant CAS and do not contain a constant Mach segment. Furthermore, they can be flown entirely at idle thrust, since they never exceed the 3000-ft/min descent rate as the other two do during portions of their descent. Another simplification is the absence of a deceleration segment at the bottom of the descent. One can conclude from these results that procedural complexity has a strong impact on time-control accuracy and should be carefully considered in choosing the descent profiles.

Time accuracy and fuel efficiency of the predicted and simulated profiles at the 30 n.mi. point are summarized in Table 3. By comparing the first and second columns it can be seen that all predicted times fall within the corresponding time ranges of the simulated profiles. This comparison indicates that there is no significant bias between the predicted and simulated data.

Table 3. Summary of simulation results, time (sec) and fuel (lb) to 30 n.mi. to touchdown point

Type of Profile	Time Predicted by Algorithm	Range of Times; Time Variability ()	Average Fuel Use	Range of Fuel Use; Fuel Variability ()
Baseline M 0.8/280 KCAS without profile advisories	--	890-1084 (196)	1065	945-1145 (200)
Nominal M 0.8/320 KCAS top of descent: 108 n.mi	893	880-915 (35)	1082	1064-1098 (34)
Fast M 0.84/350 KCAS top of descent: 107 n. mi.	863	854-871 (17)	1175	1169-1183 (14)
Slow 230 KCAS top of descent: 133 n.mi.	1104	1098-1104 (7)	771	764-778 (14)

The average fuel-consumption data given in Table 3 show that the slow profile is the most fuel efficient and the fast profile the least fuel efficient. The nominal profile, though considerably faster than the baseline profile, consumes only slightly more fuel (17 lb) on average than the baseline does. Thus, the trade-off between time and fuel, so important in airline

operations, favors choosing the nominal profile. However, the profile actually assigned to an aircraft by the air traffic scheduler will depend on the availability of a conflict-free time slot at the time of descent.

In addition to tests of the tail-wind condition reported herein, head-wind and zero-wind conditions have recently also been tested. Preliminary analysis is yielding results that are generally consistent with the tail-wind conditions. Also, the time variability between the 30-n.mi. mi. point and touchdown was investigated for both a straight-in and a standard-approach pattern, the latter consisting of downwind, base, and final segments. Analysis of results for these conditions is still in progress.

Pilots participating in the simulation generally reacted favorably toward the profile-descent advisory concept. The pilots cited as the primary benefit the accurate specification of the top-of-descent point in the presence of complex altitude-dependent wind profiles. Moreover, the pilots considered the advisories as unobtrusive and all profiles as comfortable to fly.

The experience of this study has identified the following three guidelines for achieving accurate time control. First, descent procedures provided by advisories should be simple to execute and familiar to pilots. Second, aircraft performance and atmospheric conditions should be accurately represented in the advisor algorithm. Third, pilots should be briefed on the characteristics of the advisories and the requirement to execute them accurately.

The time accuracies achieved in the simulation would be adequate for a time-based ATC system if they could be duplicated in practice. However, uncertainty in the knowledge of the actual wind profile and inevitable lapses in pilot attention to the profile tracking task will result in larger errors than obtained in the simulation. One can attempt to estimate such time errors from analysis of ATC radar tracking data during an aircraft's descent. Then, an updated speed advisory can be issued near the midpoint of the descent to minimize these errors. With the addition of such a midpoint advisory, control of arrival time within $\pm$20 sec appears to be feasible.

CONCLUDING REMARKS

Studies completed to date indicate the essential feasibility of achieving the major performance objectives of a time-based, traffic-management concept. Air traffic control simulations have demonstrated that a time-based system used in conjunction with appropriate procedures, computer aids, and information displays provides an efficient method for controlling a complex mix of traffic, including both high- and low-performance aircraft as well as various percentages of 4D-equipped aircraft.

Time control offers significant benefits even at low-percentage mixes of equipped aircraft by using advisories to help maintain unequipped aircraft on an accurate time schedule. Thus, traffic in the complex final-control sector flows more orderly and is easier to control when time control methods are in use. Although the system operates internally in a time-based mode, controllers need not be aware of this situation and retain the ability to operate in their traditional distance-spacing mode.

Piloted simulations have demonstrated the effectiveness of profile-descent advisories to control the descent time of unequipped aircraft. An accuracy at the time-control point of ±20 sec, which a time-based system needs to be effective, appears attainable with the descent advisor designed according to the methods outlined in the paper.

A combined ATC and piloted-simulation test of the concept is planned for 1987. If these tests confirm performance predictions, the FAA and NASA plan jointly to conduct operational evaluations of the concept at the Denver En-Route Air Traffic Control Center.

REFERENCES

1. Tobias, L., "Time Scheduling a Mix of 4D Equipped and Unequipped Aircraft," NASA TM 84327, Feb. 1983.

2. Alcabin, M., Erzberger, H., and Tobias, L., "Simulation of Time Control Procedures for Terminal Area Flow Management," American Control Conference, June 1985, Boston, MA.

3. Lee, H.Q., Neuman, F., and Hardy, G.H., "4D Area Navigation System Description and Flight Test Results," NASA TM D-7874, 1975.

4. Erzberger, H. and Chapel, J.D., "Concepts and Algorithms for Terminal Area Traffic Management," American Control Conference, June 1984, San Diego, CA.

5. Lee, H.Q. and Erzberger, H., "Time Controlled Descent Guidance Algorithms for Simulation of Advanced ATC Systems," NASA TM 84373, May 1983.

6. Tobias, L., Erzberger, H., Lee, H.Q., and O'Brien, P.J., "Mixing Four-Dimensional Equipped and Unequipped Aircraft in the Terminal Area," AIAA Journal of Guidance, Control and Dynamics, Vol. 8, No. 3, May-June, 1985, pp. 296-303.

7. Knox, C.E. and Cannon, D.G., "Development and Test Results of a Flight Management Algorithm for Fuel Conservative Descents in a Time Based Metered Traffic Environment," NASA TP 1717, Oct. 1980.

8. Menga, G. and Erzberger H., "Time-Controlled Descent Guidance in Uncertain Winds," AIAA Journal of Guidance and Control, Vol. 1, No. 2, Mar.-Apr. 1978, p. 123.

9. McCormick, Barnes W., Aerodynamics, Aeronautics and Flight Mechanics, New York, Wiley, 1979.

10. Chuen-Yeu, Chow, An Introduction to Computational Fluid Dynamics, New York, Wiley, 1979.

11. O'Brien, J.P., Willett, F.M., Jr., and Tobias, L., "Dynamic Air Traffic Control Simulation of Profile Descent and High Speed Approach Fuel Conservative Procedures," Federal Aviation Administration Technical Center, Atlantic City, NJ 08405, Final Report FAA-RD-80-12, May 1980.